Kinesin Force Generation Measured Using a Centrifuge Microscope Sperm-Gliding Motility Assay

Kirsten Hall,* Douglas Cole,* Yin Yeh,# and Ronald J. Baskin*
*Biophysics Graduate Group, Section of Molecular and Cellular Biology, and #Department of Applied Science, University of California, Davis, California 95616 USA

ABSTRACT To measure force generation and characterize the relationship between force and velocity in kinesin-driven motility we have developed a centrifuge microscope sperm-gliding motility assay. The average (extrapolated) value of maximum isometric force at low kinesin density was 0.90 ± 0.14 pN. Furthermore, in the experiments at low kinesin density, sperm pulled off before stall at forces between 0.40 and 0.75 pN. To further characterize our kinesin-demembranated sperm assay we estimated maximum isometric force using a laser trap-based assay. At low kinesin density, 4.34 ± 1.5 pN was the maximum force. Using values of axoneme stiffness available from other studies, we concluded that, in our centrifuge microscope-based assay, a sperm axoneme functions as a lever arm, magnifying the centrifugal force and leading to pull-off before stall. In addition, drag of the distal portion of the axoneme is increased by the centrifugal force (because the axoneme is rotated into closer proximity to the glass surface) and represents an additional force that the kinesin motor must overcome.

INTRODUCTION

Kinesin is a microtubule-based motor protein that uses the energy released from the hydrolysis of Mg-ATP to generate the force required to move intracellular membranes toward the fast-growing (plus) ends of cellular microtubules (Bloom, 1992) and has been shown to be responsible for centrifugal movement of pigment granules in melanophores (Rodionov et al., 1991). Despite our detailed knowledge of the kinesin-driven microtubule movement obtained through the use of light microscope motility assays (Cohn et al., 1989) and recent insights into how kinesin generates force and translates that force into movement (Block et al., 1990; Gelles et al., 1988; Gilbert et al., 1995; Hackney 1994; Howard et al., 1989; Svoboda and Block, 1993), our understanding of these processes is still incomplete.

To estimate the force developed by a kinesin molecule we developed a centrifuge microscope-based, sperm-gliding, motility assay (Hall et al., 1993). In this assay, the centrifugal force necessary to stop demembranated sperm movement over a kinesin-coated glass surface was determined. The centrifugal force effected the sperm head most strongly due to its high density (1.6 g cm^{-3}) and was transmitted to the kinesin attachment site via the axoneme. (The mass of the sperm head was necessary to produce the required centrifugal forces at the spin rate of the stage.) Because kinesin moves toward the tail or the plus end of an axoneme, bending of the axoneme generates a torque about the point of kinesin attachment. (Under certain conditions, as we will discuss, the sperm axoneme functions as a lever arm, magnifying the effects of the centrifugal force. This results in pull-off before stall.)

Using this assay, we observed sperm movement during a 2-min observation window at a fixed centrifugal force. We then increased the centrifugal force successively, observing the sperm movement at different forces until the sperm were observed to pull off. Whereas sperm moving in the same direction as the centrifugal force stalled, sperm moving in a direction opposite to the centrifugal force always pulled off before stalling. We reported an estimate of maximum kinesin force that was lower than that found by workers using kinesin-coated beads and microtubules in a laser trap-based assay (Kuo and Sheetz, 1993; Svoboda and Block, 1994). We obtained higher force measurements using our sperm and kinesin preparations in a laser trap-based assay. In this communication we present our recent force measurements and discuss our understanding of the basis for the low values of force observed in our centrifuge microscope-based, sperm-gliding assay.

EXPERIMENTAL PROCEDURES

Sample preparation

Sea urchin kinesin (SUK) was purified from sea urchin eggs by modifications of published procedures (Buster and Scholey, 1991). 200 ml cytosol was treated with hexokinase and glucose, centrifuged to sediment actomyosin, then supplemented with taxol (15 mM), guanine tri-phosphate (GTP) (1 mM), and sodium tripolyphosphate (10 mM). The resulting kinesin-microtubule complexes were sedimented through a sucrose cushion, washed in Mg^{+2}-free buffer, and kinesin was eluted by centrifugation in Mg-ATP. The eluate was filtered through a 0.45-μm syringe filter, concentrated to 2 ml in a centriprep-30, and fractionated on a 1.6 × 90-cm column of Biogel A1.5 M. Kinesin was pooled and bound to microtubules formed from bovine PC tubulin in the presence of adenyl-5′-yl imidodiphosphate, pelleted, eluted using Mg-ATP, and finally sedimented on a 5-ml 5–20% sucrose density gradient (300,000 g, 8.5 h). Fig. 1 shows an SDS-PAGE gel of the resulting highly purified sea urchin egg kinesin (100–200 μg).

Received for publication 26 February 1996 and in final form 25 September 1996.

Address reprint requests to Dr. Ronald J. Baskin, Department of Molecular and Cellular Biology, University of California—Davis, Storer Hall, Davis, CA 95616-8755. Tel.: 916-752-1554; Fax: 916-752-1554; E-mail: rjbaskin@ucdavis.edu.

0006-3495/96/12/3467/10 $2.00

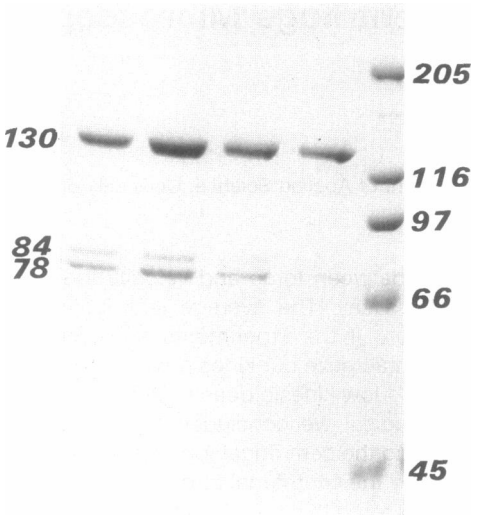

FIGURE 1 SDS-PAGE of sucrose density purified sea urchin kinesin.

Bovine brain kinesin was purified from fresh bovine brains (Bloom et al., 1988), which were stored on ice no longer than 2 h before removal of the meninges. The brains were homogenized in 1.5× volume of PMEG (85 mM K_2 PIPES, 15 mM Acid PIPES, 0.5 mM EDTA, 5.0 mM EGTA, 2.5 mM Mg SO_4, 0.9 M glycerol, 0.02% NaN_3, 1 mM DTT, 0.1 mg/ml soybean trypsin inhibitor, 0.1 mM PMSF, 10 μg/ml pepstatin, 20 μg/ml aprotinin, 10 μg/ml leupeptin, 1 mg/ml $TAME_i$ pH 6.9.) (Buster and Scholey, 1991) buffer with protease inhibitors in a Waring blender for three 10-s pulses at medium speed. The homogenate was spun at 8,000 *g* for 10 min and the resulting supernatant was spun at 100,000 *g* for 60 min to produce the high speed supernatant (HSS). Bovine brain kinesin was prepared from bovine HSS as described above for sea urchin kinesin with the following modifications. Because of the large volume of bovine brain HSS (>600 ml), the hexokinase/glucose actomyosin depletion step was omitted and the initial kinesin-microtubule binding was induced only with sodium tripolyphosphate. All kinesin samples were first assayed within 48 h of the start of the purification.

Sea urchin sperm were demembranated by treatment with Triton X100 in a high salt solution by modification of published procedures (Gibbons and Fronk, 1972). They were incubated in a demembranating solution for 5 min and then washed in a high salt buffer (PMEG with .5 M KCl, pH 8.1) to inactivate the dynein-mediated sperm motility. The demembranated sperm were checked for intact, nondamaged axonemes using video-enhanced differential interference contrast microscopy.

Preparation of the assay cell

A coverslip was hydrated in a moist chamber for ~2 min and was then coated with 2 μl of 5 mg/ml casein. The casein solution was prepared by gently agitating 5 mg/ml casein in water for 30 min at room temperature, passing the solution through a 0.2-μm filter, and finally centrifugating at high speed for 20 min to separate residual lipid from the casein. A kinesin solution (18 μl) was mixed with Mg-nucleotide (3 μl) and then gently applied to the casein-coated coverslip, so as not to disturb the coating. The coverslip was then incubated in the moist chamber for 3–5 min to allow kinesin to bind to the surface. This incubation time is probably sufficient, as noted by Hunt and Howard (1993) who estimated that the number of kinesin molecules bound to a surface will saturate within 120 s. The coating has been estimated to be ~8 nm thick, allowing kinesin that is bound to the coverslip to extend beyond the casein coating. We also assume that the kinesin is bound directly to the glass, because kinesin does not bind to casein in solution and other proteins may be used to aid in the binding of kinesin to a coverslip (Howard et al., 1989). We assume that the casein is providing a cushion that allows kinesin to bind to the glass surface without being denatured or interfered with by other kinesin molecules. The optimal concentration of casein was determined experimentally; and we have found that this concentration varies for different motor proteins. The optimal concentration of casein that allows us to use dilute sea urchin kinesin while maintaining motility is 0.33 mg/ml.

The sample cell consists of two coverslips that are separately prepared and then joined into a sandwich configuration. Three microliters of the demembranated sperm solution was gently layered onto the kinesin-coated coverslip and allowed to sit ~2 min to allow the dense demembranated sperm to diffuse down to the kinesin coating. During this incubation of the coverslip with the kinesin-nucleotide solution, the second uncoated glass coverslip was placed on the ledge in the sample cell holder where silicon grease had previously been applied to provide a seal for the coverslip. An ATP-regenerating system consisting of 2 μl each of creatine phosphate (10 units/ml) and creatine phosphokinase (50 mM) was placed on this uncoated coverslip. Finally the kinesin-nucleotide-demembranated-sperm-covered coverslip was placed on top of the ATP-regenerating-system-covered coverslip that was sitting on the cell holder. The coverslips were sealed with a solution of valine, lanolin, and paraffin that had been heated to 35–37°C. This prevented fluid evaporation as well as leakage once the cell was spun in the centrifuge microscope. This procedure brought the total volume of the cell to 30 μl, slightly higher than a conventional motility assay cell. (The reason for having some solution on each coverslip is to limit air bubbles in the assembled cell.)

Centrifuge microscopy

We assayed the kinesin-driven movement of demembranated sea urchin sperm (*Litichinus pictus*) over a coverslip mounted into a rotating microscope stage (diameter of rotation, $2r$ = 10.5 cm) of a Zeiss video micro

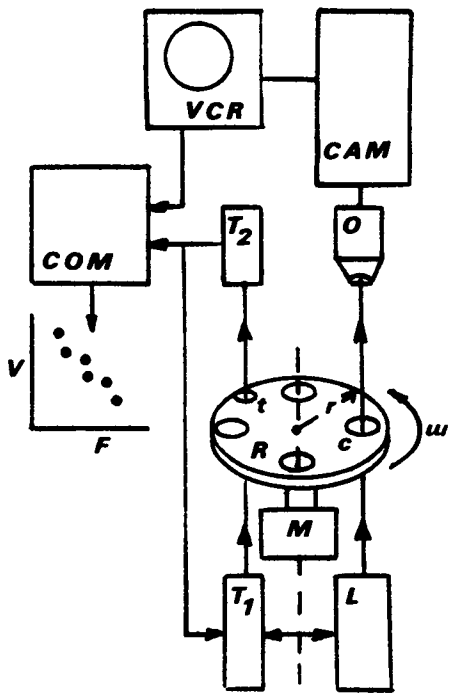

FIGURE 2 A schematic diagram of the centrifuge microscope depicting the signal pathways in the experimental system. The strobe light flashes, illuminating the rotating motility assay cell (triggered by the pulse and timing delay unit). The light beam passes through the microscope objective into the camera. The camera output is directed into the image processing computer.

scope equipped with a 40×, long working distance objective (numerical aperture = 0.75). The 10-ns stroboscopic light source (Xenon Corp. Model 437 Nanopulser) was triggered to flash in synchrony with the rotating stage by a photonic sensor control unit (Fig. 2). Motion of the sperm head was analyzed through an Imagen signal enhancer and recorded on a video recorder, and the data captured by a frame grabber were processed using the public domain software NIH IMAGE v.1.45. Using our ability to follow a single sperm head through changing applied centrifugal forces, velocities were measured from distances measured in time-sequenced captured frames.

To appreciate the nature of forces operating on the sperm head that is rotating at an angular frequency ω on the turntable-like microscope stage, we must consider an inertial frame of reference and a rotating frame of reference (Taylor, 1963). Within the fixed, inertial frame of reference, a test particle (sperm in this case) at a radial distance r from the axis of rotation will experience an inward radial acceleration, $\mathbf{a}_i = \omega \times (\omega \times r)$ (centripetal acceleration), which keeps the particle on a circular path. The equation of motion in this inertial frame of reference is thus given by $\mathbf{F} = m\mathbf{a}_i = m\omega \times (\omega \times r)$, where m is the mass of the particle being rotated. For this particle to remain stationary in the rotating frame of reference, we have a balance of forces: $\mathbf{F} - m\omega \times (\omega \times r) = 0$. An outwardly directed (centrifugal) force is present.

If instead of remaining fixed in the rotating frame of reference, the particle actually moves with a constant radial velocity, $\mathbf{v}_r$, relative to the turntable coordinates, then the velocity of a particle in the inertial reference frame is given by

$$\mathbf{v}_i = \mathbf{v}_r + \omega \times \mathbf{r}.$$

Correspondingly, the acceleration in the stationary reference frame is

$$\begin{aligned}\mathbf{a}_i &= (d\mathbf{v}_i/dt)_i \\ &= (d\mathbf{v}_r/dt)_r - \omega \times \mathbf{v}_i \\ &= \mathbf{a}_r + 2(\omega \times \mathbf{v}_r) + \omega \times (\omega \times \mathbf{r}).\end{aligned}$$

In the inertial frame of reference, the total forces felt by the particle can be written as

$$\mathbf{F} = m\mathbf{a}_i = m(\mathbf{a}_r + 2(\omega \times \mathbf{v}_r) + \omega \times (\omega \times \mathbf{r})) \quad \text{or,}$$

$$\mathbf{F}_{rot} = m\mathbf{a}_r = \mathbf{F} - 2m(\omega \times \mathbf{v}_r) - m\omega \times (\omega \times \mathbf{r}) = 0$$

The quantity $-2\ m(\omega \times \mathbf{v}_r)$ is the Coriolis force, directing a force component transverse to the motional direction, r, and $-m\omega \times (\omega \times r)$ is the centrifugal force pushing the particle away from the center of the turntable. Because the velocity of particle movement in the rotating frame is much smaller than the angular velocity of rotation, the Coriolis force is much smaller than the centrifugal force. (i.e., 3×10^{-4} pN)

The viscous drag force, given by $\mathbf{F}_d = -f\mathbf{v}_r$ where the viscous drag coefficient, f, is multiplied by the velocity of the particle, is directed opposite to the velocity of motion in the resting frame of reference. The viscous drag coefficient depends on the size and shape of the particle being moved, and the viscosity of the solution the particle is being moved through. For the purpose of calculating the viscous drag force that opposes kinesin-driven motility we modeled a demembranated sperm as a combination of a spherical head with viscous drag coefficient of $f_h = 6\pi\eta r_h$ and a long thin oblong tail with viscous drag coefficient along the axis of the axoneme equal to $f_t = 4\pi\eta a/[\ln(2a/b) - 1/2]$ (Broersma, 1963), where b is the radius of the tail and $2a$ its length. Using this model for a demembranated sperm, the viscous drag resisting the kinesin-driven motion ranges between 0.03 and 0.15 pN for kinesin-driven velocities between 1.0 and 0.2 μm/s, where we have used $\eta = 0.04$ poise, the demembranated sperm tail length, $2a = 40\ \mu$m, the demembranated sperm tail width, $2b = 0.10\ \mu$m, and the radius of the sperm head, $r_h = 1\ \mu$m.

Because we were measuring forces applied to demembranated sperm being moved by kinesin in a rotating motility assay through a buffer, we modified the mass term using the definition of volume density, $m = \rho V$, where ρ is the volume density of the particle relative to its surrounding medium, and V is the volume of the particle. We took the volume density of the sperm to be 1.6 g cm^{-3} based on the estimates of DaSilva et al. (1992) for bull sperm and the volume of the sperm as 4.2 μm^3. Typical rotational speeds ranged from 0 to 4000 revolutions/min, generating forces on the sperm heads of up to 26 pN. The maximum variance of the applied centrifugal force, due to intrinsic fluctuations in the rotor speed, was ±0.02 pN in the 2-min measurement intervals.

For each preparation of kinesin, we repeated the experiments for 3 consecutive days, completing four experiments/day. Over this period we observed no change in the efficiency of kinesin-generated ATP hydrolysis nor any significant decrease in kinesin motility. The velocity corresponding to zero force is an average of at least 15 measurements made of kinesin-driven motility under unloaded conditions. All the other points on each curve are the measurements (for each run) of the movement of a single demembranated sperm, which was tracked through the varying values of applied centrifugal force. In all experiments we selected for sperm that were most strongly attached and moving. This technique significantly reduces the measurement variation seen in our previous work (Hall et al., 1993). We only chose sperm that were moving within a plus or minus 10° arc of the centrifugal force vector. When we applied a high concentration of kinesin, we observed sperm moving in all directions irrespective of the direction of applied force. However when the experiments were performed under conditions of the minimum concentration of applied kinesin that supports motility, sperm were only moved by kinesin with or against the centrifugal force vector. In fact, most of the sperm moved by kinesin under these minimum conditions were in the direction of the force. However we observed a small number moving against the force (indeed we selected just such sperm) despite the fact that the motor heads of the kinesin molecules may have swivel-like properties (Hunt and Howard, 1993). Each symbol on the curve represents an average of three consecutive days' experiments. The subsequent force-velocity data were fit to a straight line.

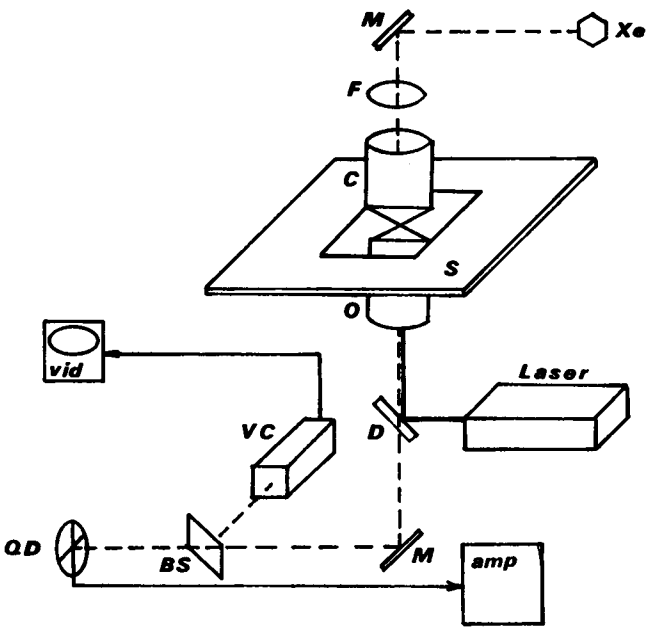

FIGURE 3 Diagram of laser trap. The dashed lines represent imaging pathways, the solid line represents the laser beam path. M indicates mirrors, C the condenser, O the objective, D a dichroic mirror, Xe the Xenon light source, BS the beam splitter, S the microscope stage moveable in the x-y plane, F a filter, Laser, the laser source, QD the quadrant photodetector, VC the video camera, and amp the amplifier and computer system.

Optical trapping

Force generated by bovine brain kinesin was measured using an optical trap (Fig. 3) located at the Beckman Laser Institute (University of California, Irvine, CA). The instrument consists of a Coherent Innova 100 argon laser (12.2W, 512 nm, 34.9 A), which powers a Coherent 899 Ti:Sapphire ring laser (1.7 W, 750 nm). The emitted beam, gated by an Unblitz Electronic Model SD-1000 shutter drive timer, passes through a manual polarizer, which regulates trap strength, and is directed through the upper camera port of a Zeiss microscope, through a Neofluor 100 objective (numerical aperture = 1.30), and into the assay slide. The motility assay image was obtained using a MTI 68 camera. The image was improved using a Hammamatsu Argus 10 image processor, viewed on a Conrac video monitor, and recorded using a Panasonic VHS video recorder.

The trap was calibrated with both 1-μm beads and whole demembranated sperm at a distance of 6–10 μm away from the underside of a casein-coated coverslip in the buffer used for the motility assay. (The proximal edge of the sperm head was 1–4 μm from the coated surface.) Calibration was performed by moving the object (bead or sperm), for 2 mm at various speeds until the sperm (or bead) was pulled out of the trap. The trapping force was calculated using Stokes law and the previously calculated drag coefficients for demembranated sperm (Hall et al., 1993). This calibrated movement was obtained using a Zeiss MSP 65 xy stage controller operated by an IBM XT computer. The resulting calibration curve (Fig. 4) was used to calculate the optical trapping force that prevented movement of the sperm (or bead).

To measure the minimum force necessary to trap a demembranated sperm head, a moving sperm head was trapped at a high (20 pN) force. Trapping force was then lowered in 1–2 pN increments until the kinesin force was large enough to overcome the trapping force and the sperm head was pushed out of the trap.

Calculation of minimum functional density

Because we incubated a solution of kinesin on a coverslip, there were only a certain percentage of kinesin that binded to the coverslip in a functional manner. The minimum functional density of kinesin was measured, in an initial series of experiments using microtubules, by lowering the concentration of kinesin until the functional kinesin molecules behaved as if they were spaced on coverslips such that every time a sheared, 5-μm-long microtubule left one kinesin, another kinesin was positioned to bind to the microtubule. This situation may be modeled as a grid of kinesin molecules spaced apart from each other by the average length of the microtubules. This experiment was then repeated using demembranated sperm, which were ~40 μm long. Based on the dimensions of these constructed grids of kinesin and an assumption that the axoneme of the demembranated sperm may fall randomly at any angle to the natural coordinates of the kinesin grid, we arrived at a probability distribution for the number of kinesin molecules interacting with a demembranated sperm at any time. This approach and the resulting probability distribution (Poisson) were discussed by Howard et al. (1989). Using this method, we estimated the presence of 1–2 functional kinesin molecules for about every 6,000 added to the assay (Table 1). The probability of two kinesins interacting with a sperm tail is 0.80; for three kinesins, it is 0.15; for six kinesins, it is 0.025; and for eight kinesins, it is <0.025. These calculations have implications for the assay with the fully concentrated kinesin as well, suggesting that we probably have 3–10 kinesin molecules generating motility along a given axoneme, and not the hundreds one would expect from the number of tubulin sites available along the axoneme.

We observed, during the initial determination of minimum functional density using a video-enhanced differential interference contrast (DIC) microscope, microtubules rotating about a point of attachment. This observation provides further evidence that we have, on average, one or two kinesin molecules per sperm. We then applied the same concentration/μm length of microtubule of kinesin to an assay containing demembranated sperm. Although we estimated that the average functional density of kinesin was such as to produce only one kinesin molecule per sperm, we had never observed demembranated sperm rotating about a point as we did with isolated microtubules. It is likely that this was due either to the inability of Brownian forces to overcome the viscous resistance of moving an entire demembranated sperm, or to the fact that our experimental protocol selects for sperm that are moved by two or more kinesin molecules.

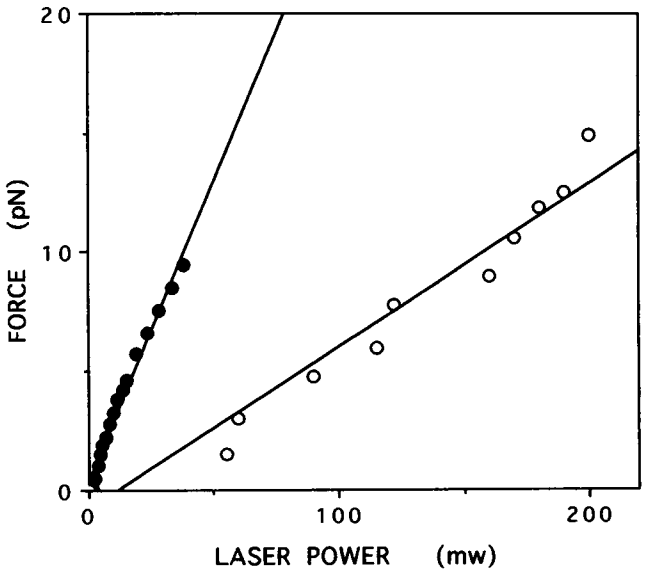

FIGURE 4 Calibration of the laser trap. Trapping forces (pN) were determined at different values of laser power expressed as a voltage proportional to the angular setting of a polarizer. A motorized stage was moved at different (constant) velocities and the force on the demembranated sperm (○) (or bead (●)) was calculated using the Stokes equation. The curve obtained using demembranated sperm was used in determining the force generated by bovine brain kinesin.

Observations of kinesin-driven demembranated sperm motility

We observed demembranated sperm being moved under conditions favoring single molecules of kinesin using video-enhanced DIC microscopy. Under these conditions the apparent single point of kinesin-axoneme attachment was easily observable as it moved toward the tail end of the sperm, pushing the sperm head-first until the sperm moved beyond the location of the kinesin and often was observed to move away from the coverslip. When kinesin was moving demembranated sperm, the sperm

TABLE 1 V_{max}, K_m, and amount of kinesin (ng) required to obtain one functional molecule per square micron for each of the six sea urchin kinesin preparations studied

Date	V_{max} (μm/sec)	K_m (μM)	Amount of protein for 1 mol/ μm^2 (ng)
12/21/93	.674	81.9	603.7
1/7/94	.547	57.5	475.5
2/4/94	.663	65.3	452.8
2/17/94	.653	62.8	532.7
3/16/94	.654	73.9	409.1
4/11/94	.650	60.1	614.4

V_{max} and K_m were obtained using a video enhanced DIC microscope and microtubules obtained from bovine brain tubulin.

head bent down away from the kinesin-coated coverslip, and the demembranated sperm tail was generally straight. We had never observed demembranated sperm with damaged or kinked tails being moved by kinesin. Furthermore, when there were no kinesin molecules coating the coverslip, portions of the demembranated sperm simply executed Brownian motion.

Observations of sperm moving against the centrifugal force vector in the centrifuge microscope also showed the sperm head bending away from the coverslip (~4–8 μm as determined by the movement necessary to refocus the objective). As the sperm continued to move it was observed to then pull off of the kinesin-coated surface. Large bends before pull-off were never observed, and we believe this is because of the fact that bending (proportional to developed force) is a function of the third power of the length (see Discussion). Thus only a small amount of bending occurred before pull-off.

RESULTS

Velocity of sperm movement was plotted as a function of applied centrifugal force. As centrifugal force increased (Fig. 5), velocity of sperm movement decreased until the sperm were abruptly pulled off. Pull-off forces varied from 0.40 pN to 0.75 pN and pull-off occurred before stall of the sperm. In these experiments, a minimum density of kinesin was adsorbed to the glass surface and 1 mM ATP was maintained by a regeneration system. The data shown are from three runs of the same protein preparation. Table 2 lists data averaged from three consecutive days for each of six different sea urchin kinesin preparations. In each case the kinesin-driven velocity decreased linearly as the centrifugal force increased. The slope of the force-velocity curve averaged −0.84 ± 0.16 μm/s/pN. The average, extrapolated value of P_o is 0.90 ± 0.14 pN.

TABLE 2 Slope of the kinesin force-velocity curve for low and high density kinesin experiments in the presence of 1 mM MgATP

	Low density		High density	
Date	Slope	P_o (calculated)	Slope	P_o (calculated)
12/21/93	−.811	.904	−.536	1.27
1/7/94	−.695	.905	−.737	.970
2/4/94	−.707	1.08	−.488	1.47
2/17/94	−.732	1.03	−.774	.905
3/16/94	−1.06	.760	−.703	1.15
4/11/94	−1.02	.734	−.895	1.18
Average =	−.83 ± .16	.90 ± .13	−.68 ± .15	1.16 ± .20

A linear regression analysis was applied to the data from six experiments done over a 3-day period on each kinesin preparation. (Data were corrected at each velocity for the drag force.) Low density concentrations were determined as described in the Experimental Procedures section. That this concentration was indeed at or near the minimum was confirmed by attempting to further lower the kinesin concentration incrementally until motility was lost altogether. In each preparation the lowest possible kinesin concentration was used increasing the probability that one (or at most two) protein molecules were acting on a single axoneme.

A similar experiment is shown in Fig. 6, the only difference being that a high density of kinesin was adsorbed to the glass surface. Velocity of sperm movement decreased with increasing centrifugal force in a manner similar to what was seen using a minimal density of kinesin, however pull-off force increased to an average of ~1.06 pN (range = 0.8–2.25 pN). The estimated average value of P_o was 1.16 ± 0.20 pN whereas the slope was −0.69 ± 0.15 μm/s/pN. The

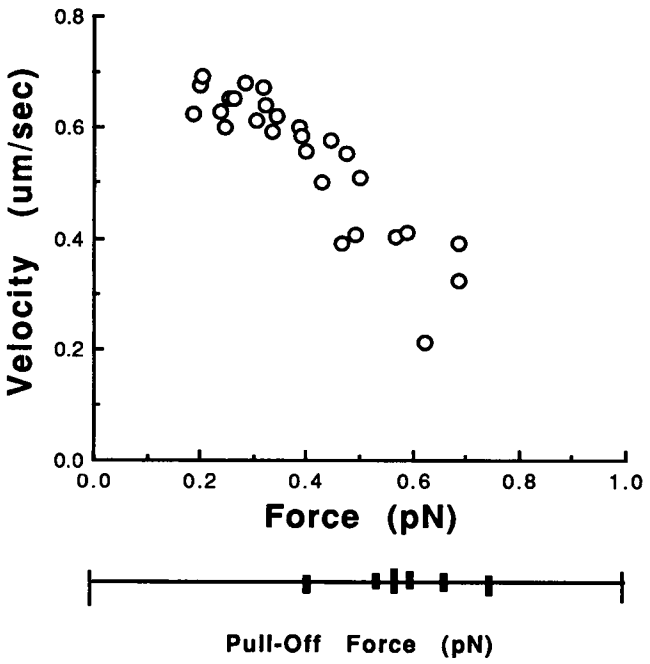

FIGURE 5 Force-velocity relationship for sea urchin kinesin. A low density preparation of kinesin was applied to the centrifuge microscope rotor cell and 1 mM ATP was maintained by a regeneration system. The data presented are from six separate runs all using kinesin from the same preparation. The pull-off forces plotted below the graph represent the minimum force that was able to induce pull-off of the demembranated sperm from the kinesin-coated surface. The (extrapolated) isometric forces, P_o, obtained by linear regression analysis of the data as well as the fitted slopes are listed in Table 2.

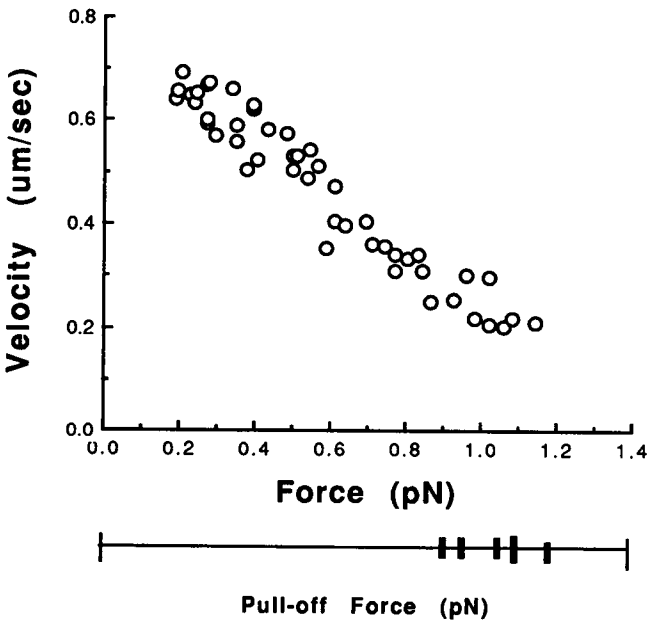

FIGURE 6 Force-velocity relationship for sea urchin kinesin obtained from a high density preparation ([ATP] maintained at 1 mM). Estimates of P_o and slope (see above) are listed in Table 2.

data from six kinesin preparations are summarized in Table 2. These data show that despite more molecules of kinesin interacting with a sperm axoneme, the decrease in velocity with increased centrifugal force (slope) is about the same as when fewer (one or two) kinesin molecules are driving the sperm.

In another experiment, we determined a force-velocity relationship (at low kinesin density) but increased force to just below pull-off. At that point we lowered force and measured velocity at these lower forces (Fig. 7). The numbers next to the data points indicate the order in which the measurements were made. The resulting curve shows repeat velocities in the same range as those found initially at similar (or near similar) values of centrifugal force. Thus we conclude that the force-velocity curve is reversible (until pull-off). Because the lever arm is lengthening from point to point the reversibility suggests that the lever arm length has no effect on kinesin velocity. All of the data in Fig. 7 are from the same demembranated sperm.

Force-velocity curves were also obtained in the presence of 0.1 mM ATP. The estimated value of P_o (maximum isometric force) was 1.47 ± 0.46 pN, similar to what was measured at an ATP concentration of 1 mM. At low kinesin density the slope of the curve was similar to what was measured at an [ATP] of 1 mM (average value of −0.74; see Table 3) but the average pull-off force was higher, ~0.98 pN. Pull-off forces were determined for 1 mM, 0.1 mM, and zero-added [ATP] (Table 4). (We estimated that <3 μM ATP was carried over from the kinesin preparation stages.) Pull-off force also increased as [ATP] was decreased to a value of 2.9 pN measured with zero-added ATP (low kinesin density). We argue that this is not due to any effect of [ATP] on the kinesin motor, but rather is due to an effect of [ATP] on axoneme stiffness. The stiffness of a demembranated axoneme has been shown to depend on [ATP] (Okuno and Hiramoto, 1979), and our analysis shows that pull-off force is a function of axoneme stiffness.

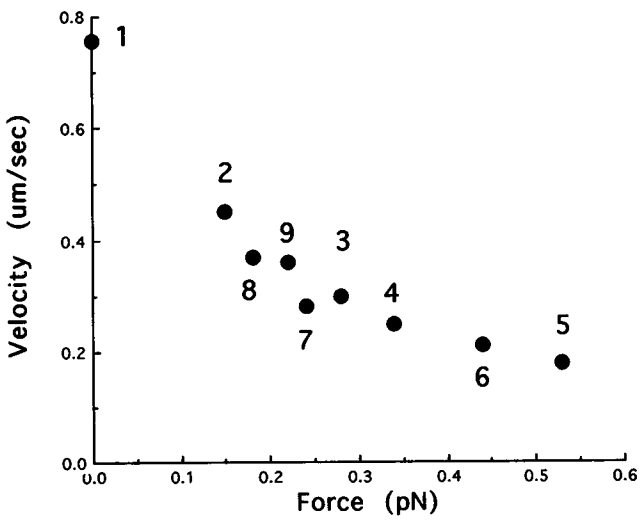

FIGURE 7 Reversibility of the force-velocity data. The data presented in this graph were obtained in the numbered order to show that, before pull-off, the velocity of sperm movement is a function of the force applied to the kinesin-coated surface, and a similar velocity is developed at a given force whether that velocity is reached by increasing or by decreasing the applied centrifugal force. All of the data were obtained from one kinesin preparation and the [ATP] was maintained at 1 mM.

TABLE 3 Slope of the kinesin force-velocity curve for low and high density kinesin concentrations in the presence of 100 μM MgATP

	Low density		High density	
Date	Slope	P_o (calculated)	Slope	P_o (calculated)
12/21/93	−.762	1.92	−.631	.901
1/7/94	−.753	1.51	−.609	.912
2/4/94	−.701	1.00	−.595	.928
Average	−.739	1.47	−.612	.914
Error	±.032	±.461	±.018	±.014

Data were calculated using a linear regression analysis on data corrected for solution drag. Data are from six experiments done on each different kinesin preparation. Low density concentrations of kinesin were determined as in Table 2.

The force-velocity curve for sperm moving in the same direction as the centrifugal force presents an interesting contrast to the counter-directional force results. In this case (Fig. 8), although velocity of movement decreases with increasing load, sperm do not pull off but instead are observed to stall at a force near to 1 pN (low kinesin density, 1 mM [ATP]). Decreasing the [ATP] to as low as 30 μM and allowing for the effect of low [ATP] on the rate of unloaded shortening, no significant change in the slope of the force-velocity curve or in the stall force was observed. We believe that this stall force is dependent upon the frictional force developed as a result of centrifugal force pulling the sperm head into the kinesin-coated surface. Further, it is likely that the slope of the curve is also influenced by drag of the sperm head upon the glass surface.

Laser trap-based assay

The low values of P_o derived from the centrifuge microscope data required that we examine the difference between the centrifuge microscope assay and the optical trap assay. We proceeded to estimate the force developed in our assay system using the optical trap-based technique. We found that demembranated sperm heads could be held, without apparent damage, in our laser trap. We were then able to estimate the amount of force that bovine brain kinesin molecule(s) needed to generate to move the sperm head out of the trap. (Experiments done using sea urchin kinesin and a less precisely calibrated laser trap yielded similar results).

We estimated that, at a low density of kinesin, a force of 4.34 ± 1.5 pN (N = 50) was required. This value is comparable to the nearly 5.0 pN measured by Svoboda and Block (1994). In some experiments the axoneme was observed to wind around the trapped head, which was able to rotate in the laser trap.

TABLE 4 Pull-off forces determined in each of the six kinesin preparations at low and high protein density with 1 mM MgATP, 100 μM MgATP, and zero-added MgATP

	Low density		High density		Zero ATP	
Preparation	1 mM MgATP	100 μM MgATP	1 mM MgATP	100 μM MgATP	Low density	High density
12/21/93	0.44 (3)	0.82 (3)	0.94 (3)	3.4 (3)		
1/7/94	0.51 (3)	0.72 (3)	0.79 (3)	3.7 (3)		
2/4/94	0.53 (3)	0.95 (3)	0.96 (3)	2.1 (3)		
2/17/94	0.52 (3)		0.96 (3)			
3/16/94	0.44 (3)		0.58 (3)		2.9 (2)	11.5 (2)
4/11/94	0.50 (3)		0.71 (3)			
Average	0.49 ± 0.04 (18)	0.83 ± 0.12 (9)	0.82 ± 0.16 (18)	3.07 ± 0.85 (9)	2.9 (2)	11.5 (2)

DISCUSSION

The major results of our centrifuge microscope sperm-gliding assay are: 1) when sperm were moved against the centrifugal force, pull-off occurred before sperm stall, and 2) the slope of the force-velocity curve obtained by this technique was steeper than that found by Svoboda and Block (1994).

We will show that the above results may be explained using the following hypothesis. Centrifugal force acting on the sperm head is transferred via the axoneme to the kinesin attachment site. A torque is developed at that site that tends to pull the axoneme away from kinesin. (The demembranated axoneme stiffness itself is a function of the [ATP]). Further, the slope of the force-velocity curve is influenced by drag of the axoneme (particularly its distal portion) near the casein-coated glass surface, which results in a different slope (steeper) than found by investigators using a laser trap-based assay. The lower estimate of kinesin force found in our centrifuge microscope-based assay results from drag and bending of the sperm axoneme. In the next section we will show that a force of ~5 pN is, in fact, generated in our assay.

Forces and torques in the gliding-sperm assay

In modeling a sperm axoneme, we have assumed that the demembranated sperm has an axoneme stiffness coefficient, EI, between 1 and 4×10^{-22} Nm^2, depending on the ATP concentration (Okuno and Hiramoto, 1979). We will analyze the forces developed and the torque balance in the presence of a motor protein force and an oppositely directed centrifugal force acting on the sperm head (Fig. 9; see Table 5 for parameter values). There are two significant drag forces. One is from the sperm head moving in solution, F_{d1}, where $F_{d1} = f_d\, v$, with f_d as the Stokes coefficient for the particle in the particular solvent. We let $f_d = 6\pi\eta a$, where η is the solution viscosity and a is the radius of the sperm head. The other drag force is due to the distal portion of the axoneme moving near or against the wall, F_{d2}. When the axoneme is not contacting the coverslip, the frictional drag coefficient will be described by the Broersma equation. When in direct contact with the coverslip, this drag force will be described by $F_{d2} = k\, F_N$, where F_N is the normal force exerted by the coverslip against the distal end of the axoneme, and k is the frictional coefficient between the coverslip and the axoneme. The flexibility of the axoneme

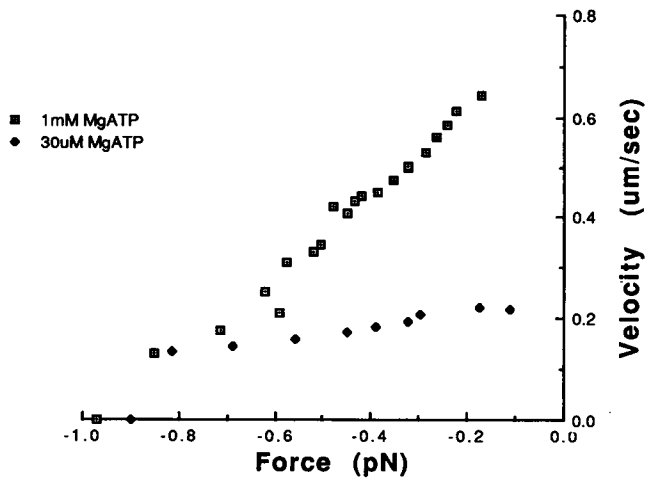

FIGURE 8 Force-velocity relationship obtained for sea urchin kinesin when derived from sperm moving in the same direction as the applied centrifugal force. Experiments were done at an [ATP] of 1 mM and 30 μM.

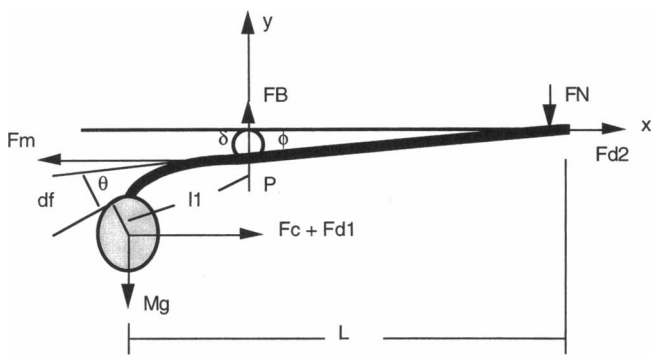

FIGURE 9 Diagram of forces acting on a sperm being moved by a kinesin molecule against an applied centrifugal force. The kinesin molecule is represented by the small circle at point P. Centrifugal force (F_c) and drag forces (F_{d1} and F_{d2}) pull the sperm in the directions indicated by the arrows. Kinesin motor force (F_m) pushes the sperm in the opposite direction. Axoneme segment l_1 acts as a lever arm and a torque is developed at point P.

TABLE 5 Numerical parameters

$l_1 = 4 \times 10^{-6}$ m to 36×10^{-6} m
$L = 40 \times 10^{-6}$ m, a constant
$\delta = 2 \times 10^{-8}$ m, a constant
$\eta = 1$ cp (centipoise) $= 10^{-3}$ Pa (Kg/ms)
$a = 1 \times 10^{-6}$ m, the radius of the sperm head (approximate)
$f_d = 6\ \pi\eta a = 6\ \pi\ 10^{-3} \times 10^{-6}$ Ns/m
$v = 0.6 \times 10^{-6}$ m/s
$M = (\rho - \rho_o)\ V$, where ρ_o = density of the solution = 1 g cm^{-3}
ρ = density of the sperm, 1.6 g cm^{-3} = 1.6×10^3 kg m^{-3}
$V = (4\pi/3)\ a^3 = 4.2 \times 10^{-18}$ m^3
$g = 9.8$ m/s^2 is the gravitational constant

will allow bending of the l_1 portion of the axoneme. The angle of bending will be labeled θ. We define the bending force as W, where:

$$W = \mathrm{Mg}\cos(\theta + \phi) + (F_c + F_{d1})\sin(\theta + \phi) \quad (1)$$

Note that both the applied force and the buoyancy-corrected gravitational force will contribute to the bending force W. We need to consider the force balance and the torque balance about the point of kinesin attachment to the axoneme, point P.

For x-component force balance, we have

$$F_m = F_c + F_{d1} + F_{d2} \quad (2)$$

For y-component force balance, we have

$$F_B = \mathrm{Mg} + F_N \quad (3)$$

The torque about the point P then becomes

$$l_1\ W = (L - l_1)\ F_N\cos\phi + \mathrm{d}F_{d2} \quad (4)$$

The following relationships apply:

1) The length of the axoneme $L = l_1 + l_2$

2) the angle ϕ is constrained by the condition

$$\sin\phi = \frac{\delta}{(\mathrm{L} - \mathrm{l_1})} \quad (5)$$

3) The deflection due to the nonrigid nature of the axoneme is given by

$$d_f = \frac{W}{3El} l_1^3 \quad (6)$$

4) $W = \mathrm{Mg}\cos(\theta + \phi) + (F_c + F_{d1})\sin(\theta + \phi)$

Because $\delta = 20$ nm, while the smallest distance of $l_1 = 1000$ nm, and $L = 4000$ nm, we can assume that $\sin\phi \sim 5 \times 10^{-4}$, and will be negligible. We therefore set $\phi = 0$.

Using $W = \mathrm{Mg}\cos\theta + (F_c + F_{d1})\sin\theta$, and $d_f = l_1 \sin\theta$, we find that

$$\sin\theta = \frac{W}{3El} l_1^2 = \frac{l_1^2}{3El}(\mathrm{Mg}\cos\theta + (F_c + F_{d1})\sin\theta).$$

Defining $C = l_1^2/3\ El$, we obtain

$$\tan\theta = \frac{C\,\mathrm{Mg}}{1 - C(F_c + F_{d1})} \quad (7)$$

We note that when $C\ (F_c + F_{d1}) = 1$, $\tan\theta =$ infinity, $\theta = \pi/2$. We calculated the force developed tending to pull off the sperm as a function of l_1 for different applied centrifugal forces. Using the relationship between kinesin force and the velocity of microtubule motion (Svoboda and Block, 1994), we see that given θ and F_c, W (Eq. 1) is obtained uniquely. This, in turn, allows us to obtain a value for F_N by using the torque balance equation (Eq. 4). Finally, from the y-direction force balance equation (Eq. 3), we obtain F_B, which is the minimum binding force needed to hold the kinesin-axoneme system together. Hence overcoming this force will produce pull-off of the sperm head. Throughout this analysis, we used an EI stiffness range from 1×10^{-22} Nm^2, to 4×10^{-22} Nm^2, which is ~5 to 20 times that of the single microtubule measured by Gittes et al. (1993).

We calculated the force tending to pull the sperm off the kinesin surface as a function of the length of the bending arm of the axoneme, l_1, when $F_c = 1$ pN, and for stiffness (EI) values of 1, 2, and 4×10^{-22} Nm^2. For the least stiff axoneme ($EI = 1 \times 10^{-22}$ Nm^2), the developed force reaches a maximum at $l_1 = 20$ μm because it then bends past 90° and sufficient force (5pN) to pull off the sperm is not developed. As the axoneme stiffens, the developed force is greater at longer l_1 values. For example, when $EI = 4 \times 10^{-22}$ Nm^2, the kinesin-axoneme binding point is at ~35 μm when sufficient force for pull-off is developed. It is reasonable to expect that at pull-off, the force needed approaches that of the rigor value (>5 pN). Furthermore, a sperm will not pull off the axoneme at a lower centrifugal force because the maximum length of axoneme (~40 μm) is not long enough to generate the required torque .

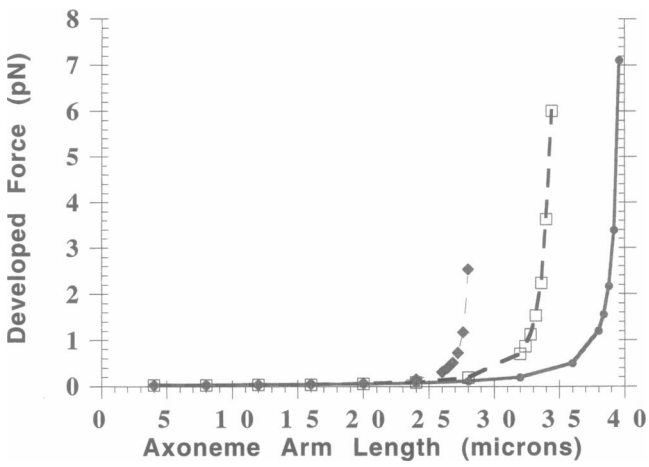

FIGURE 10 Developed force (F_B) as a function of axoneme arm length (μm). $EI = 4 \times 10^{-22}$ Nm^2. Curves are for $F_c = 0.5$ pN (●), 1.0 pN (□), and 1.5 pN (◆).

Maintaining an assumed stiffness of $EI = 4 \times 10^{-22}$ Nm^2 we also varied F_c values (Fig. 10) and looked for the variation of the pull-off force point versus the length of the axoneme. What we found is that even with $F_c = 0.5$ pN, the probability of pull-off before stall is high because the length l_1 at which binding force would exceed 5 pN is <40 μm. For higher F_c forces, the pull-off position (i.e., the axoneme position that would allow a pull-off force >5 pN to be developed) on l_1 is shorter, assuring an even higher probability of pull-off.

The major conclusion from this analysis is that centrifugal forces in the range of 0.4–1.2 pN when applied through a 30- to 40-μm lever arm (sperm axoneme) can generate forces in excess of 5 pN, and it is this effect that causes sperm to pull off from the kinesin-coated surface. The higher pull-off force found using high density kinesin preparations is consistent with the binding of more than one kinesin molecule to the axoneme. It is also apparent that stiffening of the axoneme, which would occur at a lower [ATP], would result in a requirement for a slightly higher centrifugal force (as was indeed found) to generate the force required for sperm pull-off.

Axoneme drag force

The second major result of the centrifuge microscope-based assay was the steep slope of the force-velocity curve, that is, the rapid decrease in velocity as centrifugal force (load) is increased. The reason for this, in light of the preceding assay, is obvious. The same force tending to pull the sperm away from the kinesin molecule (or molecules) will be pushing the distal portion of the axoneme against the casein-coated glass surface. As the axoneme is moved forward, this force will induce a drag on the axoneme that the motor will need to overcome for movement to occur. Thus at the same time the motor is resisting pull-off induced by the centrifugal force acting on the sperm head, it must also overcome drag in the distal portion of the tail (axoneme).

To estimate the magnitude of this drag effect, we compare the drag coefficient when a rod of radius a and length L is far removed from a wall and when it is at a distance $h \sim a$ away from the rigid wall (Brennen and Winet, 1977). For the coefficient without wall effects, the conventional Broersma (1963) equation gives:

$$f_s = \frac{2\pi\eta\, ds}{\ln(L/a) - (1/2)}$$

where ds is the elemental length along the axis of the thin rod, L is the overall length and a is the rod radius. If, on the other hand, the rod is at a distance h away from a rigid wall such that $a < h < L/2$, then Katz et al. (1975) showed that

$$f_w = \frac{2\pi\eta\, ds}{\ln(2h/a)}$$

We note that if $h = a$, then

$$\frac{f_w}{f_s} = \frac{\ln(L/a) - (1/2)}{\ln 2}$$

If $L = 40$ μm and $a = 0.1$ μm, $f_w/f_s = 7.96$. This means that at a distance of 0.1 μm from the surface, the wall effect will increase the viscous drag by 7.96 times that of the solution drag coefficient. Consequently, the drag force, f_{d2} is ~8 times that of the solution drag force.

It is of interest to note that should h become smaller than a (say $h = 0.505a$) and if the Katz et al. (1975) description of the wall effect is still valid, then the drag force becomes ~553 times that in the solution. Such a drag effect would act as a strong braking force.

If, instead, we use our previous relationship, $F_{d2} = kF_N$, then it is the wall drag coefficient, k, that will determine the magnitude of the drag force (Gau, et.al., 1994). If k were nearly unity, F_{d2} can be similar in magnitude to F_N and the true motor force considerably greater than the centrifugal force.

Another result of drag in the distal portion of the axoneme is to make complete rotation of the axoneme around a single kinesin binding site (as is observed in microtubule motility studies) unlikely, because as centrifugal force is increased, drag force will also increase. Thus the argument of Hunt and Howard (1993) that the centrifuge microscope-based sperm-gliding assay could not, in principle, measure the force developed by a single kinesin molecule is not supported by our analysis.

Effect of kinesin orientation

We assume that the kinesin molecules in our assay are oriented in a random fashion on the glass surface. Is it possible that the forces measured in our assay were influenced by the orientation of the kinesin molecules? Ishijima et al. (1996) concluded that myosin force measurements are influenced by the motor head orientation. Maximum force was only recorded from those molecules that were optimally oriented. The situation for kinesin has not yet been resolved. Hunt and Howard (1993) have shown that the kinesin motor heads have swivel-like properties, but it has not been established that maximum force can be generated at all orientation angles. Further, recent work by Sorg and Kuo (1996) has suggested the possibility of rotation of the kinesin molecule at its attachment to the glass surface during these experiments. (It is also possible that a "hand-over-hand" mechanism of action of the kinesin motor domains allows extensive rotation of a bound microtubule due to successive release and rebinding of the two head regions). Thus it is possible that (in part) the low force values measured in our experiments result from the random, and therefore nonoptimal, orientation of kinesin molecules. This may also be the basis for the fact that the P_o for high density kinesin is only ~50% greater than for low density preparations.

We believe that the centrifuge microscope is a reliable and precise method for applying a force or load to microscopic particles, but applying the load through a sperm axoneme introduces complications due to compliance and bending. This results in the generation of a torque around the point of motor attachment, a lever arm effect between the point of centrifugal force attachment and motor attachment, and increased drag as the distal portion of the axoneme is forced nearer to the glass surface. The true motor force as well as the kinesin force-velocity relationship must be computed taking these factors into consideration, and it is clear that our earlier measurements (Hall et al., 1993) did not accurately characterize either the force-velocity curve or the maximum isometric force of a kinesin molecule.

We would like to thank Dr. Jonathan Scholey for his support and encouragement during the course of this project. This work was supported in part by a UCD collaborative research grant to Y. Yeh and R. J. Baskin.

REFERENCES

Block, S. M., L. S. B. Goldstein, and B. J. Schnapp. 1990 Bead movement by single kinesin molecules studied with optical tweezers. *Nature.* 348:348–352.

Bloom, G. S. 1992. Motor proteins for cytoplasmic microtubules. *Curr. Opin. Cell Biol.* 4:66–73.

Bloom, G. S., M. C. Wagner, K. K. Pfister, and S. T. Brady. 1988. Native structure and physical properties of bovine brain kinesin and identification of the ATP-binding subunit polypeptide. *Biochemistry.* 27: 3409–3416.

Brennen, C., and H. Winet. 1977. Fluid mechanics of propulsion by cilia and flagella. *Annu. Rev. Fluid Mech.* 9:339–398

Broersma, S. 1963. Viscous force constant for a closed cylinder. *J. Chem. Phys.* 32:1632–1635.

Buster, D., and J. M. Scholey. 1991. Purification and assay of kinesin from sea urchin eggs and early embryos. *J. Cell Sci.* 14(suppl).:109–115.

Cohn, S. A., A. L. Ingold, and J. M. Scholey. 1989. Quantitative analysis of sea urchin kinesin-driven microtubule motility. *J. Biol. Chem.* 264: 4290–4297.

Da Silva, L. B., J. E. Trebes, R. Balhorn, S. Mrowka, E. Anderson, D. T. Attwood, T. W. Barbee, Jr., J. Brase, M. Corzett, J. Gray, J. A. Koch, C. Lee, D. Kern, R. S. London, B. J. MacGowan, D. L. Matthews, and G. Stone. 1992. X-ray laser microscopy of rat sperm nuclei. *Science.* 258:269–271.

Gau, C.-S., H. Yu, and G. Zografi. 1994. Surface viscoelasticity of b-casein monolayers at the air/water interface by electrocapillary wave diffraction. *J. Colloid Interface Sci.* 162:214–221.

Gelles, J., B. J. Schnapp, and M. P. Sheetz. 1988. Tracking kinesin-driven movements with nanometre-scale precision. *Nature.* 331:450–453.

Gibbons, I. R., and Fronk, E. 1972. Some properties of bound and soluble dynein from sea urchin sperm flagella. *J. Cell Biol.* 54:365–381.

Gilbert, S. P., Webb, M. R., Brune, M., and Johnson, K. A. 1995. Pathway of processive ATP hydrolysis by kinesin. *Nature.* 373:671–676.

Gittes, F., Mickey, B., Nettleton, J., and Howard, J. 1993. Flexural rigidity of microtubules and actin filaments measured from thermal fluctuations in shape. *J. Cell Biol.* 120:923–934.

Hackney, D. D. 1994. Evidence for alternating head catalysis by kinesin during microtubule-stimulated ATP hydrolysis. *Proc. Natl. Acad. Sci. USA.* 91:6865–6869.

Hall, K., D. G. Cole, Y. Yeh, J. M. Scholey, and R. J. Baskin. 1993. Force-velocity relationships in kinesin-driven motility. *Nature.* 364: 457–459.

Howard, J., A. J. Hudspeth, and R. D. Vale. 1989. Movement of microtubules by single kinesin molecules. *Nature.* 342:154–158.

Hunt, A. J., and J. Howard. 1993. Kinesin swivels to permit microtubule movement in any direction. *Proc. Natl. Acad. Sci. USA.* 90: 11653–11657.

Ishijima, A., H. Kojima, H. Higuchi, Y. Harada, T. Funatsu, and T. Yanagida. 1996. Multiple- and single-molecule analysis of the actomyosin motor by nanometer-piconewton manipulation with a microneedle: unitary steps and forces. *Biophys. J.* 70:383–400.

Katz, D. F., J. R. Clarke, and S. L. Paveri-Fontana. 1975. On the movement of slender bodies near plane boundaries at low Reynolds number. *J. Fluid Mech.* 72:529–540.

Kuo, S., and M. P. Sheetz. 1993. Force of single kinesin molecules measured with optical tweezers. *Science.* 260:232–234.

Nishizaka, T., H. Miyata, H. Y. Yoshikawa, S. Ishiwata, and K. Kinosita. 1995. Unbinding force of a single motor molecule of muscle measured using optical tweezers. *Nature.* 377:251–254.

Okuno, M., and Y. Hiramoto. 1979. Direct measurements of the stiffness of Echinoderm sperm flagella. *J. Exp. Biol.* 79:235–243.

Rodionov, V. I., F. K. Gyoeva, and V. I. Gelfand. 1991. Kinesin is responsible for centrifugal movement of pigment granules in melanophores. *Proc. Natl. Acad. Sci. USA.* 88:4956–4960.

Sorg, B. S., and S. C. Kuo. 1996. Single kinesin molecules twisted by optical tweezers. *Biophys. J.*70:A36.

Svoboda, K., and S. M. Block. 1994. Force and velocity measured for single kinesin molecules. *Cell.* 77:773–784.

Svoboda, K., C. F. Schmidt, B. J. Schnapp, and S. M. Block. 1993. Direct observation of kinesin stepping by optical trapping interferometry. *Nature.* 365:721–727.

Taylor, E. F. 1963. Chapters 6 and 9. *In* Introductory Mechanics. John Wiley & Sons, Inc., New York. 138–147; 241–265.